

Novel imidazole-based combretastatin A-4 analogues: Evaluation of their in vitro antitumor activity and molecular modeling study of their binding to the colchicine site of tubulin

Fabio Bellina,^{a,*} Silvia Cauteruccio,^a Susanna Monti^{b,*} and Renzo Rossi^a

^aDipartimento di Chimica e Chimica Industriale, Università di Pisa, Via Risorgimento 35, I-56126 Pisa, Italy

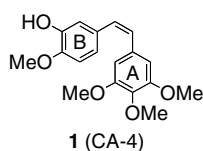
^bIstituto per i Processi Chimico-Fisici (IPCF-CNR), Area della Ricerca, Via G. Moruzzi 1, I-56124 Pisa, Italy

Received 12 July 2006; revised 18 August 2006; accepted 19 August 2006

Available online 6 September 2006

Abstract—The in vitro antitumor activity of novel combretastatin-like 1,5- and 1,2-diaryl-1*H*-imidazoles was evaluated against the NCI 60 human tumor cell lines panel. Compounds **2d** and **2g** proved to be more cytotoxic than CA-4 in tests involving their evaluation over a 10⁻⁴–10⁻⁸ range. Docking experiments showed a good correlation between the MG_MID Log GI₅₀ values of all these compounds and their calculated interaction energies with the colchicine binding site of αβ-tubulin.
© 2006 Elsevier Ltd. All rights reserved.

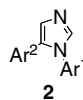
Combretastatin A-4 (CA-4) (**1**), a potent antimetabolic agent isolated from the stem wood of the South African tree *Combretum caffrum*,¹ exhibits strong antitubulin activity by binding to tubulin at the colchicine binding site.² It shows potent cytotoxicity against a variety of human cancer cell lines, including those that are multi-drug resistant³ and, most importantly, has demonstrated powerful antiangiogenesis properties.⁴



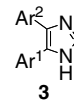
Using the X-ray structure of the tubulin–colchicinoid complex,⁵ docking studies have recently allowed the identification of reasonable binding modes of a set of different colchicine site inhibitors that included **1**, podophyllotoxin, methylchalcone, curacin A, indanocine, and nocodazole.⁶

Because of its potent cytotoxicity and structural simplicity, **1** has been envisaged as a very attractive lead

although its low aqueous solubility and *Z*-configuration pose significant liabilities. In fact, the *Z*-configured C–C double bond of **1** is prone to isomerize to the *E*-form during storage and administration thus producing dramatic reduction in both antitubulin activity and cytotoxicity.^{7,8} Therefore, considerable efforts have gone into modifying **1** and discovering its bioavailable *Z*-restricted analogues based on the bioisosteric replacement of olefinic double bond of the natural product with vicinal diaryl-substituted five-membered heteroaromatic rings including oxazole, isoxazole, thiazole, pyrazole, tetrazole, and imidazole.⁹ As far as the imidazole derivatives are concerned, it should be noted that in 2002 Wang and co-workers¹⁰ found that among a small series of 5-aryl-1-(3,4,5-trimethoxyphenyl)-1*H*-imidazoles, compounds **2a** and **2b** had comparable antiproliferative properties against the NCI-H460 non-small cell lung cancer line (63 and 61 nM, respectively) and the HCT-15 colon cancer cell line (69 and 89 nM, respectively) and very similar antitubulin activity (7.7 and 7.6 μM, respectively).



2a : R¹ = OMe; R² = NH₂
2b : R¹ = OMe; R² = OH
2c : R¹ = NH₂; R² = H



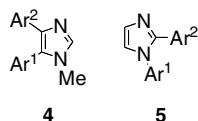
3a : Ar¹ = 3-NH₂-4-MeOC₆H₃
Ar² = 3,4,5-(MeO)₃C₆H₂
3b : Ar¹ = 3-OH,4-MeOC₆H₃
Ar² = 3,4,5-(MeO)₃C₆H₂
3c : Ar¹ = Ar² = 1-Me,5-indolyl

Keywords: Cytotoxicity; Combretastatin A-4; Colchicine; Imidazoles; Tubulin; Molecular modeling; Antitumor activity.

* Corresponding authors. Tel.: +39 0 50 2219282; fax +39 0 50 2219260 (F.B.); tel.: +39 0 50 3152520; fax +39 0 50 3152442 (S.M.); e-mail addresses: bellina@dcci.unipi.it; s.monti@ipcf.cnr.it

On the other hand, compound **2c** was inactive against NCI-H460 and HCT-15, and was not assayed for its antitubulin activity. It was also demonstrated that 4,5-diaryl-1*H*-imidazoles **3a–c** had cytotoxic and antitubulin activities significantly higher than those of compounds **2** and that incorporation of an *N*-methyl group into the imidazole ring of compounds **3** can lead to substances **4** with improved pharmacokinetic profiles, characterized by excellent bioavailability.¹⁰

Recently, in continuation of our investigations into the synthesis and evaluation of the cytotoxic activity of vicinal diaryl-substituted five-membered heterocycles, which can be considered as *Z*-restricted analogues of **1**,¹¹ we developed selective and efficient procedures for the synthesis of 1,5- and 1,2-diaryl-1*H*-imidazoles of general formula **2**¹² and **5**,^{13,14} respectively.

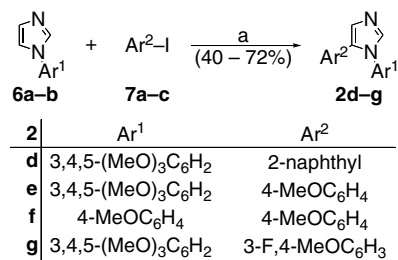


In this paper we report the evaluation of the cytotoxicity of a variety of these heterocycles. Moreover, we describe the results of molecular modeling studies performed to investigate the interactions of these CA-4 analogues at the colchicine binding site of $\alpha\beta$ -tubulin and to verify the possible relationship between their calculated interaction energies and their cytotoxicity values. In fact, some papers reporting a good correlation between cytotoxicity and experimental antitubulin activity data have been published.^{10,15} However, it has also been found that significant variations of the cytotoxicity values due to structural modifications do not affect sometimes the antitubulin activity¹⁶ and that some potent antitubulin compounds can be marginally cytotoxic.¹⁷ It should also be noted that the calculated interaction energies of compounds **2** and **5** with $\alpha\beta$ -tubulin could be very useful to identify imidazole derivatives able to cause selective damage to tumor vasculature.¹⁸

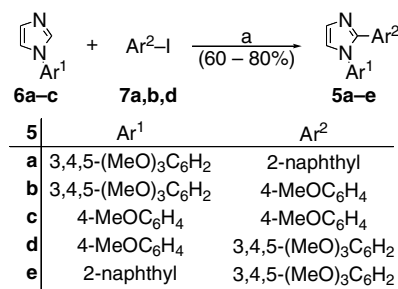
1,5-Diaryl-1*H*-imidazoles **2d–g** were regioselectively synthesized by coupling of 1-aryl-1*H*-imidazoles **6a,b** with the required aryl iodides **7** in DMF at 140 °C in the presence of CsF as the base and a catalyst precursor consisting of a mixture of Pd(OAc)₂ and AsPh₃ (Scheme 1).¹²

On the other hand, 1,2-diaryl-1*H*-imidazoles **5a–e** were regioselectively prepared by C-2 arylation of **6a–c** with the required aryl iodides **7** in DMF at 140 °C in the presence of 5 mol% Pd(OAc)₂ and 2 equiv of CuI (Scheme 2).¹⁴

Compounds **2d–g** and **5a–e** were then tested for their cytotoxic activity against the US NCI 60 tumor cell lines screening panel. The results obtained using these compounds and **1** against two selected human cancer cell lines,¹⁰ HCT-15 (MDR+) and NCI-H460 (MDR–), and the entire NCI cell panel, which are reported as



Scheme 1. Reagents and condition: (a) Compounds **7** (2 equiv), Pd(OAc)₂ (5 mol%), AsPh₃ (10 mol%), CsF (2 equiv), DMF, 140 °C, 21–90 h.



Scheme 2. Reagents and condition: (a) Compounds **7** (2 equiv), Pd(OAc)₂ (5 mol%), CuI (2 equiv), DMF, 140 °C, 48–60 h.

the mean Log molar drug concentration (MG_MID Log) for all tested human cancer cell lines, are shown in Table 1.

Some aspects of the cytotoxicity data reported in this table merit comment. First, compound **2g** proved to be the most potent imidazole derivative among the examined compounds which, save **2f** and **5c**, contained a 3,4,5-trimethoxyphenyl (TMP) group. Second, compounds **2d** and **2g** proved to be more cytotoxic than **1**, which confirms that, as previously reported, the 3-fluoro-4-methoxyphenyl and the 2-naphthyl moieties are good surrogates of the CA-4 B ring.¹⁹ Third, the 1,5-diaryl-

Table 1. Cytotoxicity of imidazoles **2d–g** and **5a–e**, and of CA-4 **1** against the NCI 60 human cancer cell lines screening panel

Compound	Cytotoxicity ^a GI ₅₀ (μM)		MG_MID Log ^a	
	HCT-15	NCI-H460	GI ₅₀	TGI
2g (NSC736359)	<0.01	<0.01	–7.40	–4.51
2d (NSC736992)	0.017	0.018	–7.14	–4.40
2e (NSC733436)	0.170	0.363	–6.59	–4.71
2f (NSC734603)	19.498	15.488	–4.80	–4.32
5e (NSC736994)	0.022	0.021	–6.86	–4.80
5a (NSC736993)	0.051	0.037	–6.82	–4.68
5d (NSC735354)	1.148	2.344	–5.45	–4.32
5b (NSC735355)	1.148	1.585	–5.34	–4.16
5c (NSC734602)	22.909	17.783	–4.76	–4.19
1 (NSC613729) ^b	<0.01	<0.01	–7.00	–5.03

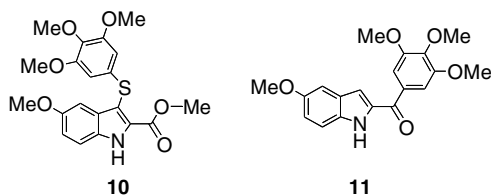
^a Evaluated over a 10^{–4} to 10^{–8} M range. These values are means of two series of cytotoxicity tests (reported in the Supporting Information).

^b <http://dtp.nci.nih.gov/dtpstandard/dwindex/index.jsp>.

1*H*-imidazoles **2d** and **2e** showed cytotoxic activities higher than those of the corresponding 1,2-diaryl-1*H*-imidazoles **5a** and **5b**, respectively. Fourth, compounds **2d** and **5a** possessing a 2-naphthyl substituent were found to be more cytotoxic than compounds **2e** and **5b**, respectively, in which the 4-methoxyphenyl moiety replaces the 2-naphthyl group. It is also worth mentioning that some of the examined imidazoles proved to be especially active against some tumor cell lines (see [Supporting Information](#)). For example, **2d** displayed Log TGI -7.53 for the colon cancer cell line HCC-2998 and the value of Log TGI of **2g** for the leukemia cell line HL-60(TB) was less than -7.54 . Thus, **2d** and **2g** were approximately 1000 times more efficacious in these cancer lines compared to the mean total growth inhibition (TGI) value in the other 59 cell lines. Finally, it should be mentioned that an *in vivo* test performed on MD-MBA-435 breast cancer cells xenotransplanted in immunodeficient mice showed that **2e** is able to inhibit significantly the tumor growth at a 150 mg/kg/day dose (52% inhibition after 25 days).²⁰

Docking studies on compounds **2d–g** and **5a–e** were then carried out to investigate the structural basis of the biological results obtained with these *cis*-locked CA-4 analogues. Thus, taking into account that the mechanism of cytotoxicity of CA-4 (**1**) and other combretastatins has been shown to involve the inhibition of tubulin polymerization by binding at the colchicine binding site of tubulin,^{9a} we directed our attention to the *in silico* determination of the total interaction energies (E_{int}) of compounds **2d–g** and **5a–e** with the colchicine binding site on $\alpha\beta$ -tubulin.

At first, the minimum energy conformations of the imidazole ligands were selected as reported in the [Supporting Information](#). Then, in order to find the best arrangement of each molecule inside the colchicine binding site, the atomic coordinates of $\alpha\beta$ -tubulin complexed with CA-4 were used as the starting point of the docking studies.⁶ Molecular docking was carried out using DOCK5 software package²¹ and the adopted docking methodology was validated by checking the energy scores obtained by docking into tubulin a representative set of ligands, namely colchicine (**8**), CA-4 (**1**), steganacin (**9**), and compounds **10** and **11**, which are included among those recently used to construct a comprehensive, structure-based pharmacophore.⁶



The docking methodology was then used for docking the minimum energy conformations of the investigated imidazole ligands into $\alpha\beta$ -tubulin. Interestingly, the top score conformers of the whole set of molecules

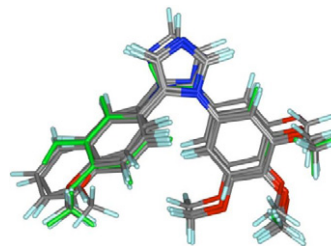


Figure 1. Arrangement of **1** (green), **2d–g** and **5a–e** inside the colchicine binding site.

had a three-dimensional arrangement of their groups similar to that assumed by **1** in its binding conformation ([Fig. 1](#)). It should also be noted that the B ring of compounds **2d**, **2e**, **2g**, and **5a**, **5b**, **5d**, and **5e** (where, as for **1**, the TMP group is represented by the A ring) was found to occupy a similar space in the colchicine binding site and was buried in all cases in the $\alpha\beta$ -tubulin structure near the Cys- β 239 residue.

On the other hand, since docking putative inhibitors in a rigid protein binding site derived from a complex with another ligand may be misleading in the identification of the correct binding mode and in the assessment of reliable binding affinities, further calculations were performed to refine the chosen adducts and find the best structural adaptation of both the protein active site residues and the ligand groups in forming the complex.

Thus, the tubulin–imidazole ligand complexes were subjected to energy minimization to relieve any unfavorable clash in the model structures and the minimized systems were used as input to short molecular dynamics simulation runs (100 ps), performed in the NVE ensemble (see [Supporting Information](#)).²² To evaluate the readjustment of the active site residues in the calculated tubulin–imidazole structures, the root mean square difference (rmsd) between the atoms of the tubulin-**1** complex and the corresponding atoms of each tubulin–imidazole model was evaluated. In the case of backbone atoms' superimposition the rmsd was lower than 0.5 Å, whereas for the side chains the maximum rmsd found was ca. 0.8 Å (for compound **5a**) suggesting that the ligand-induced conformational changes were small and, as expected, more pronounced for the side chains as compared to the main chains.

The molecular electrostatic potential (MEP) of imidazoles **2** and **5** was then examined in comparison with that of **1** ([Fig. 2](#)). Interestingly, remarkable correlations suggesting the existence of related binding mechanisms for the tubulin polymerization inhibition were found. In fact, besides having similar three-dimensional electron density shapes in their most stable binding conformations, the imidazole derivatives exhibited similar regions of positive (blue) and negative (red) electrostatic potential. It can also be noticed that in the case of **2g** the fluorine lone pairs produced a noticeable negative potential above and below the plane of the B ring, thus enlarging the negative potential lobe generated by the methoxy oxygen lone pairs. This lobe was instead smaller in **2e**

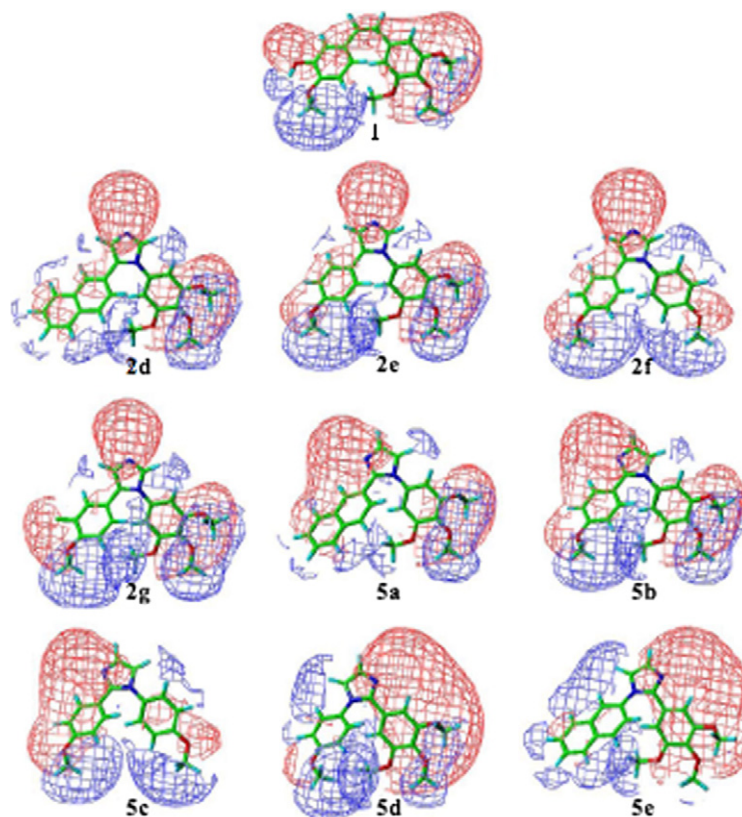


Figure 2. MEP of compounds **1**, **2d–g**, and **5a–e** produced by RESP partial charges (red and blue surfaces = -10 kcal/mol and $+10$ kcal/mol, respectively).

where the fluorine atom is replaced by a hydrogen atom. A similar, negative region was observed for the lone pairs of the OH group onto the B ring of CA-4, which, due to the presence of the hydroxyl proton hydrogen bonded to the nearby methoxy oxygen, gave rise to a somewhat compressed negative lobe. The N-3 lone pair of the imidazole ring also generated a large negative lobe, which in the case of **5d** and **5e** was enlarged by the cooperative effect of the A ring π density and its meta methoxy oxygen lone pairs. On the other hand, in the case of **5b** and **5a** the enlargement was due to the cooperation of the π density of the B ring. Analogous negative regions were observed for **2g**, **2d**, **2e**, and **2f** where the presence of the H-4 imidazole hydrogen atom prevents the enlargement of the lobe and gives rise to a very small positive region.

A negative potential was always found to be associated with the methoxy oxygen atoms of the A ring and a strong shrinking of the negative lobe was apparent for **2f** where only one methoxy group is present. On the contrary, methoxy protons produced positive lobes whose size depends on spatial arrangement and cooperative effects.

In order to quantify these qualitative predictions, the intermolecular interaction energy, which is the sum of the van der Waals and electrostatic interactions between ligand and protein, was then calculated. As shown in Table 2, the van der Waals packing between the receptor and the ligand proved to be favorable in all the models

Table 2. Total interaction energy (E_{int}), in kcal/mol, its van der Waals (vdW) and electrostatic (elec.) components and the intramolecular energy difference between the more stable conformers inside and outside the binding site (ΔE_{bind}) of each studied molecule

Compound	vdW	Elec.	E_{int}	ΔE_{bind}
CA-4	-50.529	-12.599	-63.128	
2g	-53.395	-11.181	-64.576	0.77
5a	-54.722	-6.112	-60.834	1.21
2d	-52.613	-7.729	-60.342	0.88
5e	-46.860	-12.494	-59.353	2.89
2e	-46.243	-10.956	-57.199	1.30
5d	-41.195	-12.331	-53.526	2.99
5b	-53.363	-2.232	-55.595	1.22
2f	-42.111	-4.410	-46.521	1.44
5c	-43.501	-2.405	-45.906	1.13

implying that van der Waals contacts promote binding. Compounds **2e**, **2f**, **5c**, **5d**, and **5e** had a lower number of hydrophobic contacts in comparison to the other investigated imidazoles and thus the van der Waals interaction energy was less favorable.

It was also found that the electrostatic term plays a key role in predicting the binding and that, due to additional favorable electrostatic interactions with the active site residues, greater stabilization energy was achieved for **2g** which had the lowest total energy interaction (E_{tot}) and the lowest energy difference (ΔE_{bind}) between the most stable conformers inside and outside the binding site (Table 2).

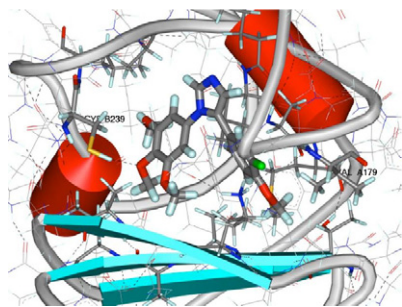


Figure 3. Compound **2g** inside the colchicine binding site. Hydrogen bonds are evidenced as dashed black lines. Secondary structure elements are represented as solid red cylinders (α -helices), solid cyan arrows (β -sheets), and solid gray ribbon (loops). Amino acids within 4.5 Å from **2g** are displayed as sticks.

It is also worth noting that the binding mode of the investigated imidazoles strongly resembled that of CA-4 **1** and that their docking revealed a consistent set of recurring interactions. As shown in Figure 3, in which compound **2g** is represented inside the colchicine binding site of tubulin, the 4-methoxy oxygen of the TMP group of compounds **2d**, **2e**, **2g** and **5a**, **5b**, **5d**, **5e** engages a hydrogen bond to the Cys- β 239 SH group and appears to be oriented so that it can interact favorably with the hydrophobic Val- β 236, Leu- β 240, Leu- β 246, Ala- β 248, Leu- β 253, and Ala- β 352 side chains, which are positioned over and below its plane (see also Tables 4 and 5 in the Supporting Information). At the bottom of the cleft which hosts the A ring the Met- β 257 side chain, owing to its sulfur lone pair, creates a negative electrostatic potential region which favorably interacts with the methyl part of the *meta* methoxy substituents, as confirmed by the value of the interaction energy with the colchicine binding site. On the other hand, the B aromatic moieties of compounds **2d**, **2e**, and **5a**, **5b**, **5d**, and **5e** were found to be located in a large pocket where their π density favorably interacts with the Asn- β 256 methylene and Ala- β 314 methyl groups (Fig. 4, and Tables 4 and 5).

In the case of **2g** (Figs. 3 and 4), the methoxy oxygen of the B ring proved to be oriented toward the methyl group of Val- α 179, and the fluorine atom was found to form a hydrogen bond with the backbone NH group of Val- α 179.

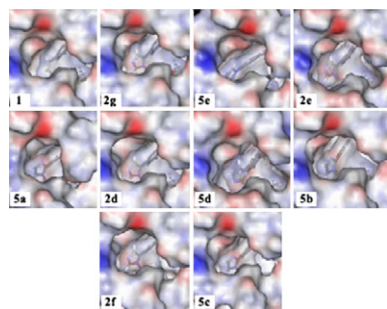


Figure 4. Compounds **1**, **2d–g**, and **5a–e** inside their binding site. Molecular surfaces colored according to the electrostatic potential (blue = positive potential region, red = negative potential region).

All the imidazole ligands were found in the same location and only a very small difference in their binding mode, due to the orientation of the imidazole moiety, was observed for **5a** and **5b**. In fact, as shown in Figure 4 and confirmed by the energy values reported in Table 3 of the Supporting Information, **5a** and **5b** had electrostatic potential matches of their imidazole ring with the nearby surface site residues less favorable than the other imidazoles. The electrostatic complementarity was not well satisfied and, to ameliorate the interaction with the site and minimize repulsion forces, these molecules were obliged to readjust the position of their imidazole rings, changing their orientation in comparison with that of the other derivatives.

Finally, it must be mentioned that even though the complementarity between the investigated imidazoles and the colchicine binding site of tubulin has proved remarkable, the existence of a set of relatively small empty pockets between the ligands and the target residues of the protein might allow an improvement of the interactions between imidazole derivatives and these regions of the binding site. The topography and volume of these cavities in the colchicine binding site, which could be occupied by substituent groups of the imidazole moiety possessing an appropriate size and polarity, can be observed, for example, in the cross section of the tubulin-**2g** binding site surfaces (Fig. 5).

In conclusion, in this study the *in vitro* antitumor activity of novel vicinal diaryl-substituted 1*H*-imidazole analogues of CA-4 has been evaluated and two 1,5-diaryl derivatives have been found to be more cytotoxic than CA-4. Moreover, a combined computational strategy consisting of molecular mechanics, rigid docking, and molecular dynamics simulations has been used to investigate the interactions of 1,5- and 1,2-diaryl-1*H*-imidazoles **2** and **5** with the colchicine binding site of $\alpha\beta$ -tubulin that is the recognized main biological target for combretastatins.⁹ The developed procedure allowed the identification of the bioactive structures of the ligands among their minimum energy conformations, their arrangement inside the binding site, and the theoretical calculation of their total interaction energy. It should be noted that some of the herewith investigated imidazoles have been shown to be characterized by high total interaction energies with the colchicine binding site and that for one of these heterocycles, **2g**, this interac-

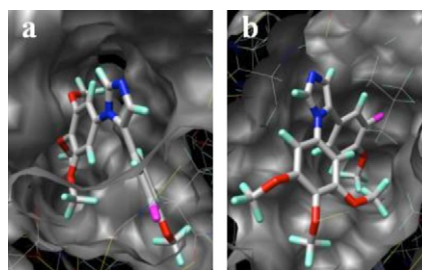


Figure 5. Cross-section of the tubulin-**2g** (a and b) binding site surfaces. Several minor cavities are visible near both the a and b moieties.

tion energy has been found to be higher than that of CA-4. The good linear correlation ($R^2 = 0.95$) between calculated interaction energies of imidazoles **2** and **5** with the colchicine binding site of $\alpha\beta$ -tubulin and their MG_MID Log GI₅₀ values, and the identification of ancillary binding site pockets, represent encouraging results, which suggest that the chosen theoretical methodology could be appropriate for the identification of compounds with increased affinity and specificity for the colchicine binding site. Finally, it is also worth noting that, as CA-4 and some other antitubulin agents have recently been shown to exhibit antivasculature disrupting activity (VDA) against tumor neovasculature at dose levels lower than those of their maximum tolerated dose,¹⁸ the calculated total interaction energies could be used to select potential lead derivatives able to cause selective VDA.

Acknowledgments

This work was supported by the University of Pisa. We are also grateful to Dr. I. Fichtner of Max Delbrück Center for Molecular Medicine in Berlin-Buch for an in vivo test of tumor growth inhibition.

Supplementary data

Complete in vitro cytotoxicity results against the NCI 60 tumor cell lines panel. Details concerning the molecular modeling procedure: conformational search (Table 3), docking and complex refinement (Fig. 6), and evaluation of the interaction energy and binding mode (Tables 4 and 5). Linear correlation graph between the calculated total interaction energy values (E_{tot}) and the experimental MG_MID Log GI₅₀ (Fig. 7). Supplementary data associated with this article can be found, in the online version, at doi:10.1016/j.bmcl.2006.08.087.

References and notes

- Pettit, G. R.; Singh, S. B.; Hamel, E.; Lin, C. M.; Alberts, D. S.; Garcia-Kendall, D. *Experientia* **1989**, *45*, 209.
- Sackett, D. L. *Pharmacol. Ther.* **1993**, *59*, 163.
- McGown, A. T.; Fox, B. W. *Cancer Chemother. Pharmacol.* **1990**, *26*, 79.
- Dark, G. G.; Hill, S. A.; Prise, V. E.; Tozer, G. M.; Pettit, G. R.; Chaplin, D. J. *Cancer Res.* **1997**, *57*, 1829.
- Ravelli, R. B. G.; Giganti, B.; Curmi, P. A.; Jourdain, I.; Lackar, S.; Sobel, A.; Knossow, M. *Nature* **2004**, *428*, 198.
- Nguyen, T. L.; McGrath, C.; Hermone, A. R.; Burnett, J. C.; Zaharevitz, D. W.; Day, B. W.; Wipf, P.; Hamel, E.; Gussio, R. *J. Med. Chem.* **2005**, *48*, 6107.
- Pettit, G. R.; Rhodes, M. R.; Herald, D. L.; Chaplin, D. J.; Stratford, M. R.; Hamel, E.; Pettit, R. K.; Chapuis, J. C.; Oliva, D. *Anticancer Drug Des.* **1998**, *13*, 981.
- Nam, N. H.; Kim, Y.; You, Y.-J.; Hong, D.-H.; Ki, H.-M.; Ahn, B.-Z. *Bioorg. Med. Chem. Lett.* **2001**, *11*, 3073.
- For reviews on the chemistry and biology of combretastatin A-4 analogues, see: (a) Nam, N.-H. *Curr. Med. Chem.* **2003**, *20*, 558; (b) Cirila, A.; Mann, J. *Nat. Prod. Rep.* **2003**, *20*, 558; (c) Tron, G. C.; Pirali, T.; Sorba, G.; Pagliai, F.; Busacca, S.; Genazzani, A. A. *J. Med. Chem.* **2006**, *49*, 3033.
- Wang, L.; Woods, K. W.; Li, Q.; Barr, K. J.; McCroskey, R. W.; Hannick, S. M.; Gherke, L.; Credo, R. B.; Hui, Y.-H.; Marsh, K.; Warner, R.; Lee, J. Y.; Zielinski-Mozng, N.; Frost, D.; Rosenberg, S. H.; Sham, H. L. *J. Med. Chem.* **2002**, *45*, 1697.
- (a) Bellina, F.; Anselmi, C.; Martina, F.; Rossi, R. *Eur. J. Org. Chem.* **2003**, 2290; (b) Bellina, F.; Falchi, E.; Rossi, R. *Atti del Convegno, P8*, XVII National Meeting of the Divisione di Chimica Farmaceutica of the Italian Chemical Society, Pisa, Italy, September 6–10, 2004; (c) Bellina, F.; Rossi, R. *Abstracts, P9*, 26th Winter Meeting of the EORTC–PAMM Group, Arcachon, France, January 26–29, 2005.
- Bellina, F.; Cauteruccio, S.; Mannina, L.; Rossi, R.; Viel, S. *J. Org. Chem.* **2005**, *70*, 3997.
- Bellina, F.; Cauteruccio, S.; Mannina, L.; Rossi, R.; Viel, S. *Eur. J. Org. Chem.* **2006**, 693.
- Bellina, F.; Cauteruccio, S.; Rossi, R. *Eur. J. Org. Chem.* **2006**, 1379.
- (a) Cushman, M.; He, H.-M.; Lin, C. M.; Hamel, E. *J. Med. Chem.* **1993**, *36*, 2817; (b) Ohsumi, K.; Hatanaka, T.; Fujita, K.; Nakagawa, R.; Fukuda, Y.; Nihei, Y.; Suga, Y.; Morinaga, Y.; Akiyama, Y.; Tsuji, T. *Bioorg. Med. Chem. Lett.* **1998**, *8*, 3153; (c) Liou, J.-P.; Chang, J.-Y.; Chang, C.-W.; Chang, C.-Y.; Mahindroo, N.; Kuo, F.-M.; Hsieh, H.-P. *J. Med. Chem.* **2004**, *47*, 2897.
- (a) Pettit, G. R.; Rhodes, M. R.; Herald, D. L.; Hamel, E.; Schmidt, J. M.; Pettit, R. K. *J. Med. Chem.* **2005**, *48*, 4087; (b) Ohsumi, K.; Nakagawa, R.; Fukuda, Y.; Hatanaka, T.; Morinaga, Y.; Nihei, Y.; Ohishi, K.; Suga, Y.; Akiyama, Y.; Tsuji, T. *J. Med. Chem.* **1998**, *41*, 3022.
- (a) Pérez-Melero, C.; Maya, A. B. S.; del Rey, B.; Caballero, E.; Medarde, M. *Bioorg. Med. Chem. Lett.* **2004**, *14*, 3771; (b) Kaffy, J.; Pontikis, R.; Carrez, D.; Croisy, A.; Monneret, C.; Florent, J.-C. *Bioorg. Med. Chem.* **2006**, *14*, 4067.
- For selected papers on the relationship between tubulin binding properties and selective damage to tumor vasculature, see: (a) Dark, G. G.; Hill, S. A.; Prise, V. E.; Tozer, G. M.; Pettit, G. R.; Chaplin, D. J. *Cancer Res.* **1997**, *57*, 1829; (b) Tozer, G. M.; Kanthou, C.; Baguley, B. C. *Nat. Rev. Cancer* **2005**, *5*, 423.
- (a) Maya, A. B.; Pérez-Melero, C.; Mateo, C.; Alonso, D.; Fernández, J. J.; Gajate, C.; Mollinedo, F.; Pelàez, R.; Caballero, E.; Medarde, M. *J. Med. Chem.* **2005**, *48*, 556; (b) Lawrence, N. J.; Hepworth, L. A.; Rennison, D.; McGown, A. T.; Hadfield, J. A. *J. Fluorine Chem.* **2003**, *123*, 101.
- This in vivo test was performed at the Max Delbrück Center for Molecular Medicine in Berlin-Buch. MDA-MB-435 breast cells were chosen since they resulted particularly sensitive in vitro to all new imidazole derivatives (see Supporting Information).
- Kuntz, I. D. *DOCK*. University of California, San Francisco, Box 2240, CA 94143-2240. <http://dock.compbio.ucsf.edu/DOCK_5/index.htm>.
- Case, D. A. et al. *AMBER 8*. University of California, San Francisco, 2002.